Mem. S.A.It. Vol. 87, 605
© SAIt 2016
Memorie della

High-precision HST proper motions of globular clusters

A. Bellini

Space Telescope Science Institute, 3700 San Martin Drive, Baltimore, MD, 21210, USA
e-mail: bellini@stsci.edu

Abstract. Photometric and spectroscopic studies over the last 15 years have revolutionized our understanding of globular clusters (GCs). We now know that essentially all GCs host multiple stellar populations that can be identified along all evolutionary sequences and are characterized by differences in light elements, He, and sometimes Fe. These findings present a number of formidable challenges for the study of the formation and evolution of GCs. The internal kinematics of multiple stellar populations is a fundamental piece of the puzzle and high-precision proper motions are the key tool to shed light on many open questions regarding GCs.

Key words. Astrometry – Proper motions – Galaxy: globular clusters: general – Stars: kinematics and dynamics

1. Introduction

Numerous observational studies have revealed the ubiquitous presence of multiple stellar populations (MPs) in globular clusters (GCs) and cast many difficult challenges for the study of the formation and dynamical history of these ancient stellar systems. Instead of being "simple stellar populations" with a single age and composition, essentially all clusters have been found to show some spread or bifurcation in their photometric sequences along their main sequences (e.g. ωCen, Anderson 1997), subgiant branches (e.g. NGC 1851, Milone et al. 2008), red-giant branches (e.g. M22, Marino et al. 2009, or even white-dwarf cooling sequences (Bellini et al. 2013). The exquisite precision and stability of the *Hubble Space Telescope* (*HST*) has made much of this possible (see Piotto et al. 2015 and references therein). These different sequences can be traced to different abundances of light elements (such as Na, O, Al, Mg observed spectroscopically; see e.g. Gratton et al. 2012, and references therein) and presumably Helium (e.g., Piotto et al. 2005) which is hard to observe spectroscopically.

These observational findings have cast a number of formidable challenges for the study of the formation and evolution of GCs: what is the sequence of events that led to the formation of MPs? What are the processes responsible for the cluster-to-cluster differences in the MP chemical and photometric properties? What is the source of gas out of which different stellar populations formed? What are the differences in the structural and kinematic properties of different stellar populations? What is the role of the formation processes and that of dynamical evolution in determining the current structural/kinematic properties of MPs?

In order to make progress toward a complete picture of the formation and evolutionary history of GCs, as well as to constrain

the possible paths for the theoretical study of these complex challenges and questions, a major effort to combine observational data is essential. Spectroscopic and photometric studies have begun to shed light on the chemical properties, number of distinct sequences and spanned range of ages of different stellar populations. These are only some of the pieces of information we need to constrain GCs formation history and to identify possible sources of gas out of which MPs formed. Structural and kinematic properties of different stellar populations are two additional *key pieces* of the puzzle, as they contain essential information to build a complete picture of formation and evolution of MP-hosting clusters.

2. Our project

There are now many GCs that have high-quality data in the *HST* archive spanning 14 years or more, and more observations are being taken all the time. We recently constructed (Bellini et al. 2014, Paper I) high-precision PM catalogs for over 20 clusters for which there exist two or more well-separated epochs in the archive, and we are extending the list to over 60 objects, thanks to the new data taken within the "HST UV Legacy Survey of Galactic Globular Clusters" treasury program (Piotto et al. 2015). Each catalog contains astrometry and photometry for thousands of stars within two arcmin of the center. The catalogs are focused on the many stars within a few magnitudes of the turnoff and have typical proper-motion errors of about 30 μas yr^{-1} (or 1.4 km s^{-1} at a typical GC distance of 10 kpc).

With our high-quality PM catalogs it is now possible to address many important topics for a large number of GCs such as:

(1) cluster-field separation, for luminosity- and mass-function analyses and the study of binaries and exotic stars;
(2) internal motions, to study in detail the kinematics and the dynamics of GCs in general and of each MP component in particular (with the aim of looking for fossil signatures of distinct star-formation events);
(3) absolute motions;
(4) geometric distance by comparing the LOS velocity dispersion with that on the plane of the sky;
(5) cluster rotation on the plane of the sky;
(6) energy equipartition, from the analysis of stellar velocity dispersion as a function of the stellar mass (e.g., Trenti & van der Marel 2013);
(7) (an)isotropy, by comparing tangential and radial components of the stellar motion;
(8) full three-dimensional cluster dynamics, when LOS velocities are also known;
(9) Intermediate-mass black hole hunting (e.g., van der Marel & Anderson 2010).

We have already started to work on some of these topics. For instance, during the development of our reduction procedures we measured the absolute PM of NGC 6681 and that of the Sagittarius dwarf spheroidal galaxy (Massari et al. 2013). In Watkins et al. (2015, Paper II), we derived consistent kinematics and structural properties of bright stars in 22 GCs. In Watkins et al. (2015, Paper III), we estimated GC dynamical distances and mass-to-light ratios. In Baldwin et al. (2016, Paper IV), we provided an average, kinematic-based mass estimate for blue-straggler stars. We have also analyzed the impact of unresolved binaries on the PM dispersion profiles (Bianchini et al. 2016), and detected a significant difference in the radial-to-tangential isotropy profile among the MPs of NGC 2808 (Bellini et al. 2015). In the next Section, we provide a brief description of one of our current projects (Bellini et al., in prep.).

3. The rotation of 47 Tuc on the plane of the sky

The rotation of the GC 47 Tuc on the plane of the sky has been measured in 2003 by using 2 WFPC2 fields diametrically opposite at about 5.′7 from the center of the cluster (Anderson & King 2003). *HST* is free to rotate around its major axis, so that when we transform stellar positions measured on different exposures into a common reference frame (to measure their PM), the transformations themselves must also take into account rotation effects. As a consequence, any real sign of intrinsic rotation of

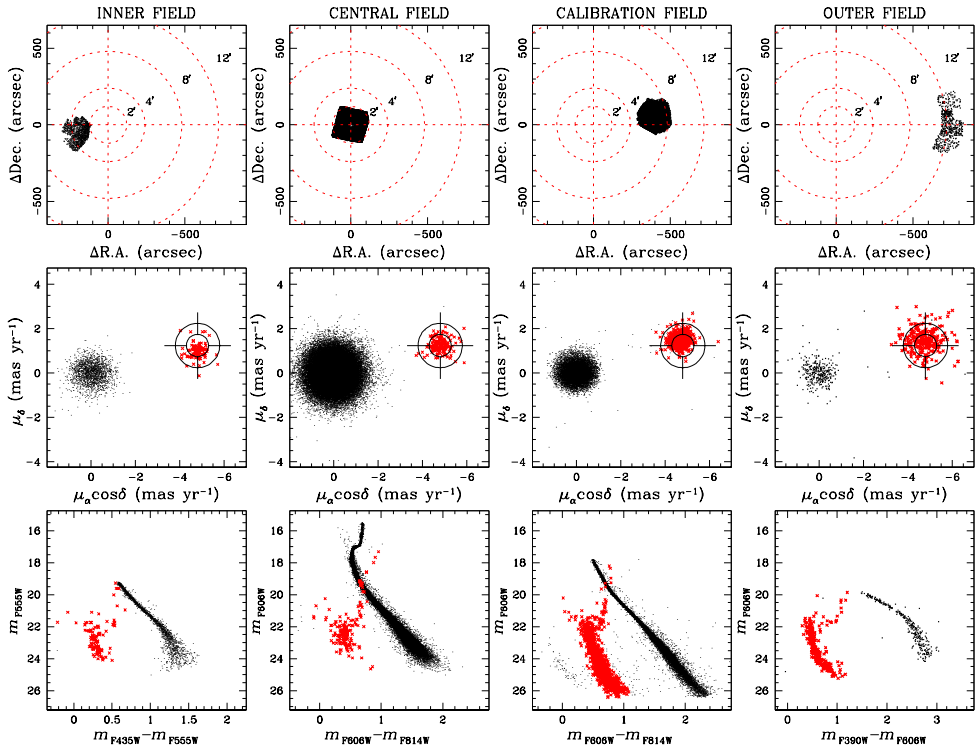

Fig. 1. From left to right: the inner field, the central field, the calibration field, and the outer field. From top to bottom, for each field: the FoV, the PM diagram, and the CMD. SMC stars are highlighted in red in the PM diagrams and in the CMDs. Concentric circles on the top panels, in red, give an idea of the radial extension of the data. The center of the crosshairs in the PM diagrams define the zero point used to compute the tangential velocity of SMC stars. See the text for more details.

47 Tuc stars on the plane of the sky is automatically masked out by the applied transformations. Anyway, there are plenty of SMC stars in the background of 47 Tuc, that obviously do not rotate around the cluster. If we measure relative PMs using 47 Tuc stars as a reference, then we can use the apparent rotation of SMC stars on the plane of the sky (due to transformation effects), invert its direction, and have a direct measure of the intrinsic rotation of the cluster. We have now extended the pioneering work of Anderson & King (2003) to a much wider field of view (FoV), longer time baseline and higher-quality PMs.

Figure 1 shows, on the top panels, the FoV of 4 *HST* fields around the center of the cluster that we have analyzed for this project. From left to right we have, respectively:

(1) the "inner" field;
(2) the "central" field;
(3) the ACS "calibration" field;
(4) the "outer" field.

Concentric circles, in red, give an idea of the radial extension of the data. The four fields are roughly aligned along the same axis, so that our cluster's rotation estimate is not sensitive to triaxial body rotation (if present). Note that stars in the outer fields are drawn with larger points, for better clarity.

The proper-motion diagrams of the four fields are shown on the middle panels of Fig. 1, in units of mas yr^{-1}, while the respective color-magnitude diagrams (CMDs) are in the bottom panels. SMC stars are selected based on both their location on the PM diagrams and

on the CMDs. We started by preliminary selecting SMC stars using generous cuts on the PM diagrams, since on this plane SMC stars are tightly clustered and well separated from 47 Tuc stars. Next, we improved our selections by rejecting all those stars that, on the basis of their location on the CMDs, were clearly not SMC stars. Our selected SMC stars are shown in red in the middle and bottom panels of Fig. 1.

We computed the barycenter of SMC stars in the PM diagram of the central field (crosshairs in Fig. 1), and kept this location fixed in the PM diagrams of the other fields. We can already see that, for the fields to the right of the cluster's center, SMC stars seem to move toward positive μ_δ, while the opposite happens for the inner field, which is to the left w.r.t. the cluster's center. This is a direct consequence of the intrinsic rotation of the cluster. We computed the tangential PM component $\mu_{\rm TAN}$ of SMC stars in different radial intervals in all 4 fields. The computed quantities (with opposite sign) as a function of the radial distance are shown in Fig. 2, with errorbars. The horizontal bars in the Figure indicate the interval over which each $\mu_{\rm TAN}$ value is computed. For completeness, we included (in red) the rotation value computed by Anderson & King (2003).

The cluster has a solid-body-like rotation within our central field. A simple least-squares fit of the form $\mu_{\rm TAN} = mr$ gives $m = -0.035 \pm 0.002$ km s^{-1} arcsec^{-1} (assuming a cluster's distance of 4.5 kpc from Harris 1996). Then, the rotation profile slowly flatten at larger radii, to reach the highest value of -6.66 ± 0.33 km s^{-1} at $\sim 390''$ ($\sim 6'.52$) from the cluster center. The measured rotation slows down to about 5 km s^{-1} in the outermost regions probed by our data.

The shape of rotation curve of 47 Tuc we have measured on the plane of the sky is qualitatively similar to that obtained by Bianchini et al. (2013) using line-of-sight (LOS) measurements. There is, though, an important difference between LOS-based and PM-based rotation profiles: the absolute value of the rotation peak on the plane of the sky is about a factor of two larger than that measured along the LOS. We are now in the process of combining PM and LoS rotation measurements to better model and constrain the real 3D orientation of the rotation axis of the cluster.

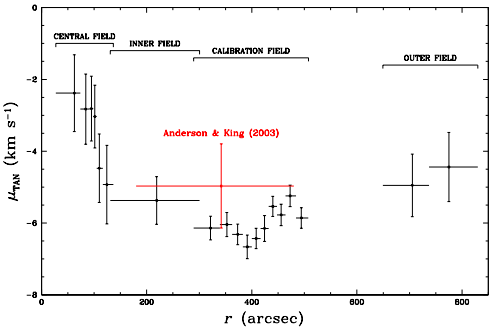

Fig. 2. Rotation of 47 Tuc $\mu_{\rm TAN}$ on the plane of the sky measured in the four fields, with errors. For completeness, we included the value computed by Anderson & King (2003). The horizontal bars indicate the radial intervals over which each $\mu_{\rm TAN}$ value is determined.

Acknowledgements. The author acknowledges support from STScI grants AR-12845 (PI: Bellini). Based on archival observations with the NASA/ESA *Hubble Space Telescope*, obtained at the Space Telescope Science Institute, which is operated by AURA, Inc., under NASA contract NAS 5-26555.

References

Anderson, J., 1997, Ph.D. thesis, Univ. of California, Berkeley
Anderson, J., & King, I. R. 2003, AJ, 126, 772
Baldwin, A. T., Watkins, L. L., van der Marel, R. P., et al. 2016, arXiv:1606.00836
Bellini, A., Anderson, J., Salaris, M., et al. 2013, ApJ, 769, L32
Bellini, A., Anderson, J., van der Marel, R. P., et al. 2014, ApJ, 797, 115
Bellini, A., Vesperini, E., Piotto, G., et al. 2015, ApJ, 810, L13
Bianchini, P., Varri, A. L., Bertin, G., & Zocchi, A. 2013, ApJ, 772, 67
Bianchini, P., Norris, M. A., van de Ven, G., et al. 2016, ApJ, 820, L22
Gratton, R. G., Carretta, E., & Bragaglia, A. 2012, A&A Rev., 20, 50
Harris, W.E. 1996, AJ, 112, 1487

Marino, A. F., Milone, A. P., Piotto, G., et al. 2009, A&A, 505, 1099
Massari, D., Bellini, A., Ferraro, F. R., et al. 2013, ApJ, 779, 81
Milone, A. P., Bedin, L. R., Piotto, G., et al. 2008, ApJ, 673, 241
Piotto, G., Villanova, S., Bedin, L. R., et al. 2005, ApJ, 621, 777
Piotto, G., Milone, A. P., Bedin, L. R., et al. 2015, AJ, 149, 91
Trenti, M., & van der Marel, R. 2013, MNRAS, 435, 3272
van der Marel, R. P., & Anderson, J. 2010, ApJ, 710, 1063
Watkins, L. L., van der Marel, R. P., Bellini, A., & Anderson, J. 2015, ApJ, 812, 149
Watkins, L. L., van der Marel, R. P., Bellini, A., & Anderson, J. 2015, ApJ, 812, 149